

Test of the Linearity of Quantum Mechanics in Optically Pumped ^{201}Hg

P. K. Majumder, B. J. Venema, S. K. Lamoreaux, B. R. Heckel, and E. N. Fortson

Physics Department, FM-15, University of Washington, Seattle, Washington 98195

(Received 13 August 1990)

Measurement of the free precession of nuclear spins in optically pumped ground-state ^{201}Hg atoms has allowed a test of Weinberg's nonlinear generalization of quantum mechanics. Shifts among the three resolved precession frequencies in the spin- $\frac{1}{2}$ system were studied as a function of the projection of spin polarization along the precession axis. Our results set an upper limit on ϵ , Weinberg's nonlinearity parameter, of $|\epsilon|/2\pi\hbar < 3.8 \mu\text{Hz}$, which corresponds to 2.0×10^{-27} of the binding energy per nucleon. This is the most stringent such limit to date.

PACS numbers: 03.65.Bz, 06.30.Ft, 32.80.Bx, 76.60.Es

Recently, Weinberg has formulated a nonlinear version of the Schrödinger equation that in lowest order reduces to ordinary quantum mechanics.^{1,2} Several groups have since reported upper limits³⁻⁵ on the nonlinearity parameter ϵ introduced by Weinberg. These results underscore the importance of precise measurements to verify the accuracy of the Schrödinger equation independently of any specific quantum-mechanical system. We report here the results of an experimental study of the spin-precession frequencies of optically pumped ^{201}Hg . The limit on possible nonlinear quantum-mechanical (NLQM) effects set by our measurement is the most stringent to date and results from a novel analysis technique.

In addition to the "ordinary" quantum-mechanical Hamiltonian, Weinberg's generalized theory contains terms proportional to powers of $\psi^*\psi$ making the overall energy dependent on the wave-function amplitude. Our discussion is limited to the discrete system described by the four ground-state Zeeman levels of ^{201}Hg ($I=F=\frac{1}{2}$) in a magnetic field. In this case, the lowest-order nonlinear Schrödinger equation takes the form

$$i\hbar \frac{d\psi_\mu}{dt} = \mathcal{H}_{\mu\mu}\psi_\mu + \frac{\epsilon}{N} \left[\sum_\nu \psi_\nu^* \mathcal{G}_{\mu\nu} \psi_\nu \right] \psi_\mu, \quad (1)$$

where $\mathcal{H}_{\mu\mu}$ is the zeroth-order energy of Zeeman level μ , N is the norm of the wave function, $\mathcal{G}_{\mu\nu}$ is a constant tensor, and $\mu, \nu \in \{\frac{3}{2}, \frac{1}{2}, -\frac{1}{2}, -\frac{3}{2}\}$. Possible terms of the form $(\psi_\nu^* \mathcal{G}_{\mu\nu\nu'} \psi_{\nu'}) \psi_\mu$ for $\nu \neq \nu'$ time average to zero in our case (i.e., when the three Zeeman frequencies are resolved, as described below).

We search for the effect of nonlinearities by measuring the precession frequency of the ^{201}Hg nuclear spins as a function of $\psi^*\psi$, in our case as a function of the cone angle of precession. We use optical pumping to polarize the spins at various angles θ relative to the final precession axis, and measure the frequency of free precession by the modulation it produces in the transmission of the pumping light. To apply Eq. (1) to our experiment we begin by rewriting the wave-function probabilities $\psi_\nu^* \psi_\nu / N$ as diagonal elements of the density matrix $\rho_{\nu\nu}^{(0)}$. The superscript indicates that the elements are defined along the initial polarization direction (pump axis). It is then convenient to re-express the individual $\rho_{\nu\nu}^{(0)}$ in a basis of orthogonal spherical tensors, T_{L0} , and corresponding multipole polarizations, defined by $\rho_{L0}^{(0)} \equiv \text{Tr}(\rho^{(0)} T_{L0})$.^{6,7} In the spin- $\frac{1}{2}$ case, the ensemble is characterized by dipole, quadrupole, and octupole polarizations. The nonlinear corrections to the energies now have the form

$$\delta E_\mu \equiv \epsilon \sum_\nu \mathcal{G}_{\mu\nu} \sum_{L=0}^3 \rho_{L0}^{(0)} T_{L0}^{\nu\nu}. \quad (2)$$

The various multipole polarizations have distinct relaxation lifetimes,⁶ γ_L , which couple differently to the incident light, allowing straightforward determination of each $\rho_{L0}^{(0)}$ and γ_L . Along the precession axis, which is rotated by an angle θ from the pump axis, the polarizations are simply given by $\rho_{L0}(\theta) = \rho_{L0}^{(0)} P_L(\cos\theta)$, where $P_L(\cos\theta)$ is the L th-order Legendre polynomial. Using the values of $\mathcal{G}_{\mu\nu}$ derived from Weinberg's rotationally invariant theory, the shifts in the observed precession frequencies in terms of the time-dependent atomic polarization moments are

$$\begin{aligned} \delta\omega_{3/2, 1/2} &= \frac{1}{\hbar} (\delta E_{3/2} - \delta E_{1/2}) = \frac{\epsilon}{\hbar} \left[-\frac{9}{\sqrt{5}} \rho_{10}(\theta, t) + \rho_{20}(\theta, t) + \frac{12}{\sqrt{5}} \rho_{30}(\theta, t) \right], \\ \delta\omega_{1/2, -1/2} &= \frac{1}{\hbar} (\delta E_{1/2} - \delta E_{-1/2}) = \frac{\epsilon}{\hbar} \left[-\frac{15}{\sqrt{5}} \rho_{10}(\theta, t) - \frac{15}{\sqrt{5}} \rho_{30}(\theta, t) \right], \\ \delta\omega_{-1/2, -3/2} &= \frac{1}{\hbar} (\delta E_{-1/2} - \delta E_{-3/2}) = \frac{\epsilon}{\hbar} \left[-\frac{9}{\sqrt{5}} \rho_{10}(\theta, t) - \rho_{20}(\theta, t) + \frac{12}{\sqrt{5}} \rho_{30}(\theta, t) \right], \end{aligned} \quad (3)$$

where $\rho_{L0}(\theta, t) = \rho_{L0}(\theta) \exp(-\gamma_L t)$, and we have omitted the "monopole" component of the polarization, $\rho_{00}^{(0)}$, which is constant.

The ^{201}Hg atoms in our experiment sample an external magnetic field from the confines of an evacuated quartz cell of asymmetric shape ($2 \times 2 \times 1$ -cm rectangular box). The ensemble-averaged electric-field gradient experienced by the atoms as they sample all cell surfaces produces a symmetric quadrupole frequency shift, $\omega_q = 50$ mHz, among the four sublevels. Because the quadrupole interaction shifts the levels in proportion to $|m_l|^2$, the single Larmor frequency is split into three. When the relaxation times are sufficiently long, this can lead to beats in the detected component of the total atomic spin. As has been observed previously,^{8,9} the size of the observed quadrupole splitting depends on the relative orientation of the magnetic field and the axis of the "cell quadrupole." When the two axes do not coincide, proper diagonalization of the total Hamiltonian shows that there can exist a nonsymmetric quadrupole splitting.^{8,9} We refer to this as a fixed "octupole" shift, ω_0 .

The optical pumping apparatus used to perform this measurement is similar to that described previously.⁷ The important features are illustrated in Fig. 1. About 1×10^{13} ^{201}Hg atoms are contained in a cell made of high-purity synthetic quartz. The cell is maintained at 400°C which increases the spin-relaxation lifetimes. Three independent coils produce a resultant magnetic field in the x - z plane that defines the quantization direction for each phase of the experiment. The apparatus is

surrounded by three layers of magnetic shielding which reduce the residual field at the cell to less than $50 \mu\text{G}$. 254-nm resonance radiation from a ^{198}Hg microwave discharge lamp is used to both optically pump and probe the atoms.

For the pumping cycle, the light is circularly polarized, either σ_+ or σ_- . The two field coils labeled B_z and B'_z are set to be equal and opposite, and the atoms are polarized along B_x . Typically, 60–90 s are required for the polarization to reach a steady-state value. At this time, a second linear polarizer and small aperture are placed in the path of the incident light. The photoelastic modulator is now turned on, and the circular polarization of the light incident on the cell varies sinusoidally at a frequency $f_0 = 42.3$ kHz. At the same time, the value of B'_z is varied adiabatically until the atomic spins point at some angle ϕ relative to the pump direction. To initiate the probe cycle, both B'_z and B_x are switched off suddenly. The atoms then precess around B_z with a Larmor frequency $\omega_L \approx 2$ Hz and with a cone angle given by $\theta = 90^\circ - \phi$. As the atoms precess, their absorption of light of a given circular polarization varies nearly sinusoidally. A solar-blind photomultiplier tube is used to detect the UV light transmitted through the cell as a function of time. A lock-in amplifier is used to demodulate the detected light at f_0 . The low-frequency output of the lock-in amplifier becomes a measure of the dipole polarization of the ensemble. Use of the photoelastic modulator reduces the $1/f$ -type noise in the final signal, and eliminates the dipole light shift.^{6,7} A computer controls the pump and probe cycles and collects digitized samples of the lock-in output. The spin precession is monitored for about 240 s (roughly 2.5 coherence lifetimes). Typical data for the case of $\theta = 90^\circ$ are plotted in Fig. 2, showing beats among the three resolved coherences.

A number of known systematic effects can cause the Larmor frequency and quadrupole splitting to drift on the time scale of our measurements. Magnetic-field changes can shift the entire three-frequency spectrum, while cell-temperature variation or changes in the quadrupole light shift^{6,7} can cause symmetric shifts of the outer two frequencies. In practice, 100- μHz run-to-run Larmor-frequency variations were observed, while drifts in the quadrupole splitting were at or below the level of our statistical noise. To isolate a possible effect attributable to nonlinear quantum mechanics from such systematic effects, we search for a frequency shift of an octupole nature that also has the appropriate exponential time dependence. Consider a quantity which is the difference between the center and average of the outer two frequencies. Except for the small effect of a nonaligned cell axis, such a residual octupole frequency shift vanishes in ordinary quantum mechanics. Furthermore, by insuring that the magnetic field and cell axis coincide for the measurements discussed here, any residual octupole shift can be made very small. Finally, such

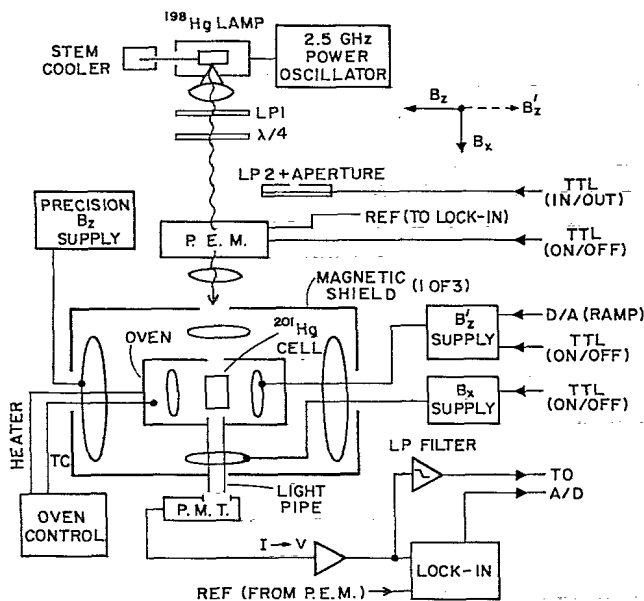


FIG. 1. Schematic of the apparatus. Abbreviations are defined as follows: TC, thermocouple; PMT, photomultiplier tube; PEM, photoelastic modulator; LP1, LP2, linear polarizers; $\lambda/4$, quarter-wave plate. Arrows on the right-hand side of the figure indicate control lines from and data lines into the computer (not shown).

a quantity is insensitive to the systematic drifts mentioned above. It follows from Eqs. (3), however, that nonlinear quantum mechanics predicts a shift of the middle frequency with respect to the outer two of the form

$$\Omega_{NL} \equiv \epsilon f(\theta, t) = \left[\frac{\epsilon \rho_{10}^{(0)}}{\hbar} \right] \frac{6}{\sqrt{5}} \cos\theta \left[e^{-\gamma_1 t} + \frac{9}{4} \left(\frac{\rho_{30}^{(0)}}{\rho_{10}^{(0)}} \right) (5 \cos^2\theta - 3) e^{-\gamma_3 t} \right], \quad (4)$$

where we have written out the angular and time dependences explicitly.

Measurements of the signal decay in the absence of precession give us γ_1 directly. Measured dipole and quadrupole relaxation times then allow us to infer a value for γ_3 . We find $1/\gamma_1 = 130(5)$ s and $1/\gamma_3 = 70(5)$ s. By measuring the relative amplitudes of the three coherences for a known precession angle, we determine that $\rho_{30}^{(0)}/\rho_{10}^{(0)} = 0.18(02)$. Residual uncertainties in these calibration parameters have no significant effect on the results of our measurement, as verified by analyzing data with altered parameter values. The absolute value of the dipole polarization $\rho_{10}^{(0)}$ was measured by first determining the fraction of detected light which is resonant with the atoms, as well as the cell absorption length (atoms unpolarized). After optically pumping with σ_+ light, a value for $\rho_{10}^{(0)}$ can be deduced from observing the change in transmitted light upon switching to σ_- . In units consistent with the form of the T_{L0} , we find a lower limit of $\rho_{10}^{(0)} = 0.30$, or about 45% of the value for a maximally polarized four-level system (all atoms in $m_I = +\frac{3}{2}$ or $-\frac{3}{2}$).

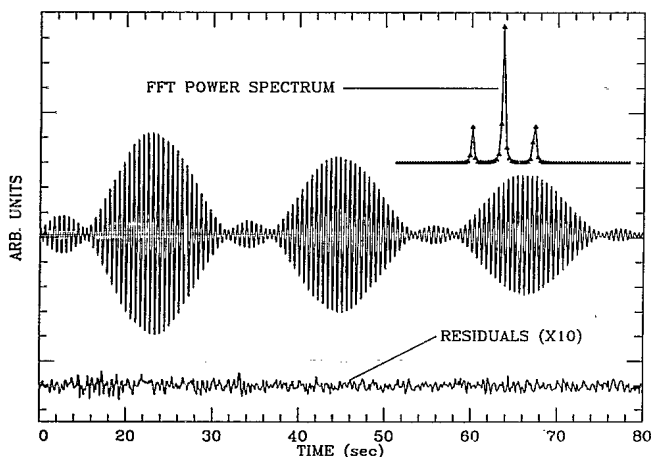


FIG. 2. Typical free-precession signal for $\theta = 90^\circ$. The signal is the output of the lock-in amplifier which demodulates the observed transmitted light intensity at the 42-kHz PEM frequency. Shown below, multiplied by 10, are the residuals of a nonlinear least-squares fit of the data by a sum of decaying cosines. Photon shot noise accounts for nearly all of the observed scatter, limiting the signal-to-noise ratio in this case to about 400 to 1. Finally, above the precession signal, a portion of its 2048-point fast Fourier transform is shown. As described in the text, we parametrize the three frequencies in terms of $\omega_L \pm \omega_q$ (outer frequencies) and $\omega_L + \omega_O + \Omega_{NL}$ (central frequency), where ω_L and ω_q are the Larmor frequency and quadrupole splitting; ω_O is a small fixed octupole shift; and $\Omega_{NL}(\theta, t)$ is the proposed NLQM shift.

Time-domain data such as that of Fig. 2 are fitted using a nonlinear least-squares-fitting routine. The fitting function is characterized by three amplitudes, corresponding frequencies, phases, and decay rates, as well as a dc background. We find that the $\rho_{1/2, -1/2}$ density-matrix element typically decays with a 90-s time constant, while the decay time for both $\rho_{3/2, 1/2}$ and $\rho_{-1/2, -3/2}$ is about 80 s. The 1.1 ratio of these decay times implies that both quadrupole and dipole relaxation mechanisms are significant here.¹⁰ With suitable redefinition of ω_L and ω_q , it is possible to parametrize the NLQM shift Ω_{NL} as a time-dependent addition to the central frequency. In practice, $f(\theta, t)$ is determined from the parameters of a given run, and ϵ becomes an additional fit parameter.

Data for "shallow" precession angles (from 15° to 45°), as well as for $\theta = 90^\circ$, were collected over a two month period yielding a total of about 3000 4-min "runs." Typical frequency uncertainties for a single run ranged from 5 to 40 μHz depending on the value of θ for that run. The fit residuals (see Fig. 2) show no evidence of features which would significantly increase the χ^2 (and hence the error bars) beyond the shot-noise-limited value. Small angles would have the largest NLQM effect, but suffer from the poorest signal to noise. Typically, the first 5–10 s of precession data were discarded to allow any fast transients associated with the field switching to decay away. Because Ω_{NL} depends only on odd multipole moments of the atomic polarization, it is odd about $\theta = 90^\circ$. Measurements at $\theta = 90^\circ$ are insensitive to the NLQM effects we seek and so become useful for the study of systematic effects such as the fixed octupole shift discussed above. Fitting the 90° data with ϵ held to zero shows that the fixed octupole shift is indeed small, and has the value $\omega_O = 2.5(0.5)$ μHz . It is possible to hold ω_O to this value during analysis of the rest of the data in which we search for a NLQM effect since this offset depends only on the direction of the precession axis, which is constant, and not on the size of the cone of precession. Data were analyzed in this way, and also by letting both ω_O and ϵ vary simultaneously in the fits. The final results based on these two analysis methods were in excellent agreement. The circular polarization of the pumping light was changed daily by rotating the quarter-wave plate by 90° . This had the effect of reversing the sign of the initial dipole and octupole polarization in the sample (while leaving the quadrupole polarization unchanged). In the analysis, this was equivalent to changing θ to $180^\circ - \theta$. Data were also taken at several different probe-light levels, and with pump and probe

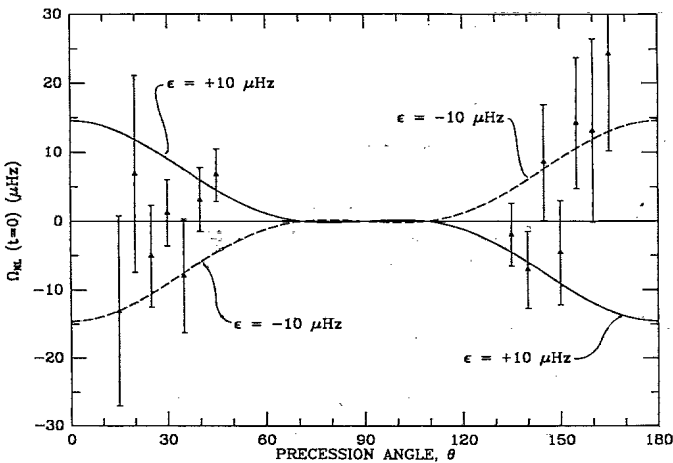


FIG. 3. Comparison of experimental and theoretical NLQM shifts at $t=0$. The theoretical curves are calculated from Eq. (3), using the measured values of $\rho_{10}^{(0)}$ and $\rho_{30}^{(0)}/\rho_{30}^{(0)}$. Data taken with σ_- pump-light polarization have been plotted with θ replaced by $180^\circ - \theta$. To deduce an experimental value for ϵ we fitted the data by a one-parameter function of the form of Eq. (4).

magnetic fields reversed.

The mean and standard deviation of ϵ values for all runs at a given precession angle and pump-light polarization (σ_+, σ_-) were computed. The χ^2 for all such sets of runs varied between 0.8 and 1.5. It is possible to express the results in terms of experimentally predicted values for $\Omega_{NL}(\theta)$ at $t=0$. Figure 3 shows these results, where we have chosen to plot σ_- results in the range of $90^\circ < \theta < 180^\circ$. Also plotted are the theoretical predictions of Eq. (4) for $\epsilon = \pm 10 \mu\text{Hz}$. Taking the *difference* of the corresponding σ_+, σ_- values allows us to place a limit on any systematic error associated with incident light polarization of $0.3 \mu\text{Hz}$, which does not contribute significantly to the final uncertainty. The residual uncertainty in the value to which we hold the fixed octupole offset contributes a systematic error of $0.4 \mu\text{Hz}$, which has been added linearly to the statistical error in the final analysis. Comparing the data and theory as suggested in Fig. 3, we find that $\epsilon/2\pi\hbar = -1.1(2.7) \mu\text{Hz}$. Thus the fraction of the binding energy per ^{201}Hg nucleon which could be due to NLQM effects is less than 2.0×10^{-27} ($3.8 \mu\text{Hz}$). This represents a factor-of-2 improvement

on the limits set by a recent measurement of the $^9\text{Be}^+$ ground-state hyperfine splitting,³ and is an order of magnitude more stringent than limits on NLQM effects in the ^{21}Ne nucleus.⁴ Our experimental uncertainties, largely limited by statistics, could be reduced significantly by increasing the relaxation time of atoms in our cell, as well as improving our light detection efficiency.

We thank F. J. Raab, who, with the support of National Institute of Standards and Technology Precision Measurement Grant No. 60NANB6D0645, was responsible for the construction and initial development of much of the apparatus used here. Helpful contributions were made by J. P. Jacobs and D. Meekhof at various stages of the experiment. Insightful comments by J. J. Bollinger concerning the manuscript were greatly appreciated. The support of NSF Grants No. PHY-8922274 and No. PHY-8451277 is also gratefully acknowledged.

¹S. Weinberg, Phys. Rev. Lett. **62**, 485 (1989).

²S. Weinberg, Ann. Phys. (N.Y.) **194**, 336 (1989).

³J. J. Bollinger, D. J. Heinzen, W. M. Itano, S. L. Gilbert, and D. J. Wineland, Phys. Rev. Lett. **63**, 1031 (1989).

⁴T. E. Chupp and R. J. Hoare, Phys. Rev. Lett. **64**, 2261 (1990).

⁵R. L. Walsworth, I. F. Silvera, E. M. Mattison, and R. F. Vessot, Phys. Rev. Lett. **64**, 2599 (1990).

⁶W. Happer, Rev. Mod. Phys. **44**, 169 (1972).

⁷S. K. Lamoreaux, J. P. Jacobs, B. R. Heckel, F. J. Raab, and E. N. Fortson, Phys. Rev. A **39**, 1082 (1989).

⁸C. H. Volk, J. G. Mark, and B. C. Grover, Phys. Rev. A **20**, 2381 (1979).

⁹Z. Wu, W. Happer, M. Kitano, and J. Daniels, Phys. Rev. A **42**, 2774 (1990).

¹⁰The ratio of coherence relaxation lifetimes would be 1.5 for pure quadrupole relaxation, and 1.0 for pure dipole relaxation. The (dipole) relaxation time for ^{199}Hg atoms (also in our cell) implies a 600-s dipole relaxation time for ^{201}Hg (assuming that the interaction scales as the square of the g -factor ratio). An additional quadrupole relaxation time of 175 s then accounts for the transverse and longitudinal decays which are observed. We have assumed in this analysis that the multipole relaxation rates γ_L are independent of M for a given L . For the case of small external magnetic fields, this "isotropic" approximation should be valid (see Ref. 6).